In Fig. 3 we see that both Miller and Kihuchi find appreciable photostar yields at the assumed threshold of 148 Mev. Kikuchi's data rise more rapidly than the predictions of the mechanism of Sec. II. $\lambda=4\times10^{-13}$ cm and $\lambda=8\times10^{-13}$ cm predict approximately the same values of $S(E)$.

Miller has evaluated $S(E)$ for two groups of emulsion elements by potential barrier argument:[2] the light elements C, N, and O, and the heavy elements Br, Ag and I. He ignores S which is present in small amounts. We include S with the light elements using the predictions of Sec. II. The results are shown in Fig. 4 for the light elements, in Fig. 5 for the heavy elements. For both groups of elements, the predictions for $\lambda=4\times10^{-13}$ cm and $\lambda=8\times10^{-13}$ cm do not differ greatly.

The values of $S(E)$ predicted by the mechanism of Sec. II agrees well with the observed $S(E)$ for the heavy element group, but is much smaller than the observed $S(E)$ for the light element group. The observed $S(E)$ may very well result from a superposition of two mechanisms, one of which is that of Sec. II, the other giving photostar cross sections which vary as A. Perhaps the deuteron model of Levinger[15] provides this second mechanism.

IV. CONCLUSION

The mesonic mechanism of Sec. II predicts a large part of the yield of photostars with three and more prongs for elements $A\gtrsim80$, but only a small fraction of the yield for elements $A\lesssim15$.

The results found in Sec. II do not differ greatly from results based on the optical model, using Eq. (1), and using formula (5) from Fernbach, Serber, and Taylor[16] for σ_{abs}. The fact that virtual mesons play only a small role in the mechanism accounts for this agreement.

I am grateful to Professor K. M. Watson for suggesting this problem and for his interest and guidance during its consideration.

[15] J. S. Levinger, Phys. Rev. **84**, 43 (1951).
[16] Fernbach, Serber, and Taylor, Phys. Rev. **75**, 1352 (1949).

PHYSICAL REVIEW VOLUME 91, NUMBER 1 JULY 1, 1953

Angular Distribution of Pions Scattered by Hydrogen*

H. L. ANDERSON, E. FERMI, R. MARTIN, AND D. E. NAGLE
Institute for Nuclear Studies, University of Chicago, Chicago, Illinois
(Received March 6, 1953)

The angular distribution of pions scattered by liquid hydrogen has been studied using the collimated pion beams from the Chicago synchrocyclotron. Differential cross sections have been measured for the laboratory angles 45°, 90°, and 135° for positive pions of energies 78 Mev, 110 Mev, and 135 Mev, and for negative pions of 120 Mev and 144 Mev. For negative pions, separate results were obtained for the elastic scattering and for the charge exchange scattering. The scattering of positive pions and charge exchange scattering of negative pions show a larger intensity in the backward direction. The elastic scattering of negative pions is mostly forward.

The results have been interpreted in terms of phase shift analysis on the assumption that the scattering is mainly due to states of isotopic spins $\frac{3}{2}$ and $\frac{1}{2}$ and angular momenta $s_{\frac{1}{2}}$, $p_{\frac{1}{2}}$ and $p_{\frac{3}{2}}$.

The experimental results are represented quite accurately by the following phase shifts expressed in degrees for the angular momentum states in the order indicated above: at 120 Mev, phase shifts ∓15, ±4, ±30 for isotopic spin $\frac{3}{2}$ and ±9, ∓3, ±2 for isotopic spin $\frac{1}{2}$; at 135 Mev, ∓14, ±5, ±38 for isotopic spin $\frac{3}{2}$ and ±10, ∓5, ±2 for isotopic spin $\frac{1}{2}$.

IN earlier communications[1,2] measurements of the total cross sections of hydrogen for both negative and positive pions at various energies were reported. In order to study in greater detail the features of the interaction between pions and protons, it appeared important to investigate also the nature and the angular distribution of the scattered particles.[3] The experiments are being carried out with the well-collimated pion beams of the Chicago Synchrocyclotron using scintillation counter techniques. This is a report on the progress of this investigation.

I. EXPERIMENTAL ARRANGEMENT

The pions are produced by a 450-Mev proton beam striking a beryllium target inside the cyclotron. Negative pions emitted in the forward direction are bent outward by the cyclotron magnetic field and emerge through a thin aluminum window from the vacuum chamber of the machine. A certain amount of focusing takes place, so that a sizeable fraction of the pions of given energy leave the cyclotron in a fairly parallel beam. The 12-foot thick steel and concrete shield which separates the cyclotron from the experiment room has

* Research supported by a joint program of the U. S. Office of Naval Research and the U. S. Atomic Energy Commission.
[1] Anderson, Fermi, Long, Martin, and Nagle, Phys. Rev. **85**, 934 (1952).
[2] Anderson, Fermi, Long, and Nagle, Phys. Rev. **85**, 936 (1952).
[3] Anderson, Fermi, Nagle, and Yodh, Phys. Rev. **86**, 793 (1952).

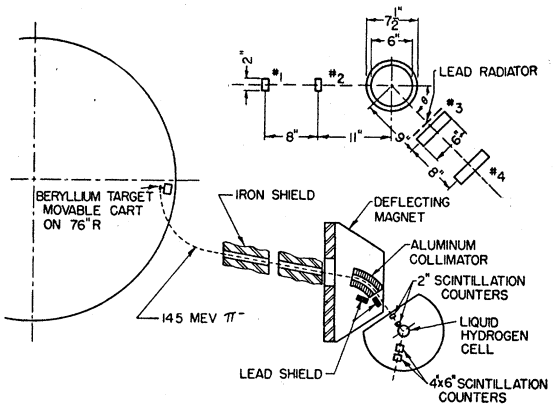

FIG. 1. General experimental arrangement. In the inset the details of the scattering geometry are given.

channels cut through it to accept a number of these beams with different energies.

On the experiment side of the shield a sector magnet deflects the pions through an angle of about 45°. The beam is purified thereby from most of the unwanted radiation (mostly neutrons) which comes through the channel.

Positive pions are obtained by reversing the direction of both the cyclotron and the deflecting magnetic fields. The proton beam in the cyclotron then circulates counterclockwise, and the positive pions which are emitted backward from this direction follow the same trajectories and have the same energy as their negative counterparts. The backward emission is unfavorable and the intensity of the positive pions which is obtained in this way is much smaller than that of the negatives.

The general arrangement is shown in Fig. 1. The pion beam is defined by passing through two 2-in. diameter liquid scintillation counters No. 1 and No. 2, and thereafter enters the hydrogen cell. The scattered particles are detected by a pair of scintillation counters, No. 3 and No. 4, arranged on a table to pivot around the central axis of the hydrogen cell. In some experiments these two counters were 4 in. in diameter; in others they were rectangles of 4 in.×6 in. A quadruple coincidence is recorded when a particle passes through the first two counters and is scattered so as to pass through the second pair. The double coincidences of the first pair are recorded at the same time. The fraction of the incident beam which is scattered is given by the ratio of the quadruple to double coincidences. The hydrogen cell was designed for rapid insertion and removal of the liquid hydrogen in order to distinguish the effect of the hydrogen from the scattering by surrounding materials. The resolving power of the coincidence equipment was fast enough (2×10^{-8} second), and the general background of stray radiation in the room was small enough, that chance coincidences were very few.

II. SCINTILLATION COUNTERS

Liquid scintillation counters were found convenient in this work because they can be made with large areas of sensitivity over which their response is quite uniform. Their speed is quite high (6×10^{-9} second). The use of low density and low Z materials makes the absorption and scattering of pions in them tolerably small. The design of the 2-in. scintillation cell is shown in Fig. 2. The cell is made of clear Lucite $\frac{3}{4}$-in. thick over all with $\frac{1}{16}$-in. thick Lucite windows. The liquid is phenylcyclohexane with 3 grams per liter of terphenyl and 10 mg per liter of diphenylhexatriene according to the prescription of Kallman.[4] The end of the Lucite cell is shaped to fit the photocathode of a 5819 tube and good optical contact is assured by a thin layer of clear silicone grease. The whole cell is wrapped in thin aluminum foil which enhances the light collecting efficiency. Phototube

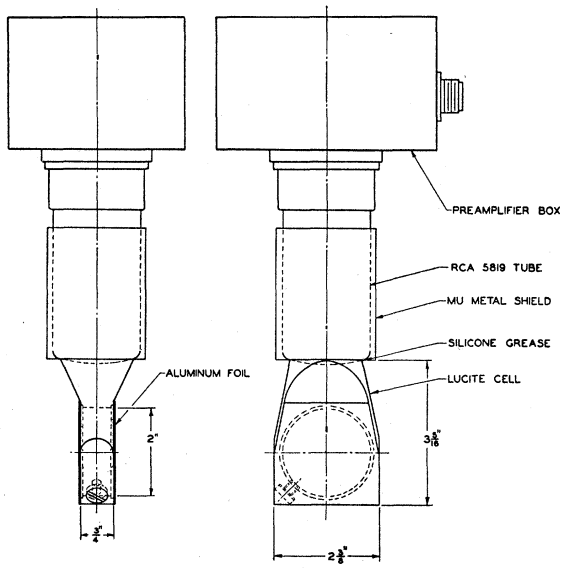

FIG. 2. Two-inch diameter scintillation counters.

and scintillation cell are light-proofed with black Scotch electric tape. An iron shield is necessary to protect the photomultiplier from the stray magnetic field of the cyclotron.

Two different types of counters No. 3 and No. 4 have been used at different times. In the earlier experiments 4-in. diameter scintillation counters were used; later the counters were changed to a newer type with a sensitive region of 4 in.×6 in. The 4-in. diameter counters were 1 in. thick over all with $\frac{1}{16}$-in. thick Lucite windows. The ends of the Lucite cell were shaped to fit the large cylindrical photocathode of an RCA C-7157 photomultiplier. The Lucite cell and the photomultiplier were enclosed in a steel box for magnetic shielding. The box was provided with $\frac{1}{32}$-in. mu-metal windows in front and in back of the sensitive area of the cell.

[4] H. Kallman and M. Furst, Phys. Rev. **81**, 853 (1951).

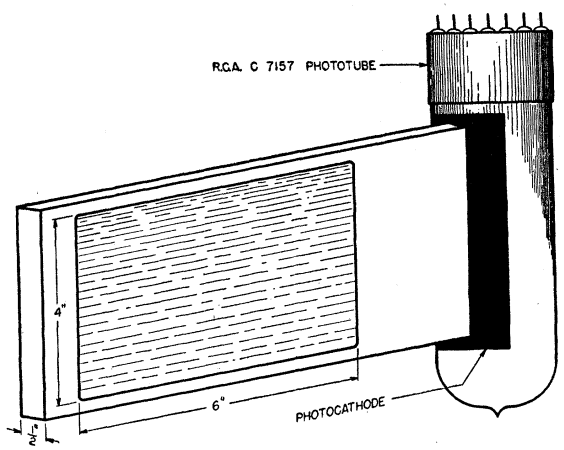

FIG. 3. Rectangular 4-in.×6-in. scintillation counters.

The design of the 4 in.×6 in. scintillation cells is shown in Fig. 3. They are also made of clear Lucite with $\frac{1}{16}$-in. thick Lucite windows. The over-all thickness is $\frac{1}{2}$ in. The ends are shaped to fit the large cylindrical photocathode of the RCA C-7157 photomultiplier. The photomultiplier is protected from the stray magnetic field of the cyclotron by a cylindrical iron enclosure not shown in the figure. The scintillation cell itself was wrapped in thin aluminum foil to improve the light collecting efficiency and to keep out stray light.

The response of both types of scintillators is uniform within 5 percent over their area. This was shown by making traverses with a narrow $\frac{1}{4}$-in. beam of Co^{60} gamma-rays across the diameters parallel and perpendicular to the photocathode and reading the anode current of the photomultiplier directly on a microammeter.

For meson counting the photomultipliers were connected to a preamplifier which incorporated a 200-ohm line, 8 feet long, to clip the pulses into a fairly square shape of 2×10^{-8} second duration. The pulses were fed to the cyclotron control room through some 150 feet of 95-ohm RG7-U cable. The pulses were amplified tenfold by means of 100-ohm distributed amplifiers and fed to the coincidence circuits.

The coincidence circuits were designed using some of the ideas of Garwin.[5] The circuit used is given in Fig. 4. It can be arranged to record either the single pulses from any given scintillator, or the double, triple, quadruple coincidences of any chosen combination, by the manipulation of suitable switches. The outputs of the first two scintillation counters were fed into the first coincidence circuit set to record doubles, and also into the second coincidence circuit set to record quadruples of all four scintillators. The coincidence circuits operate with negative pulses of 2 volts or more provided their duration is greater than 1×10^{-8} second. The photomultipliers were operated to deliver about 0.4 volt from meson pulses. With the amplification by 10, this was ample for reliable operation of the coincidence circuits.

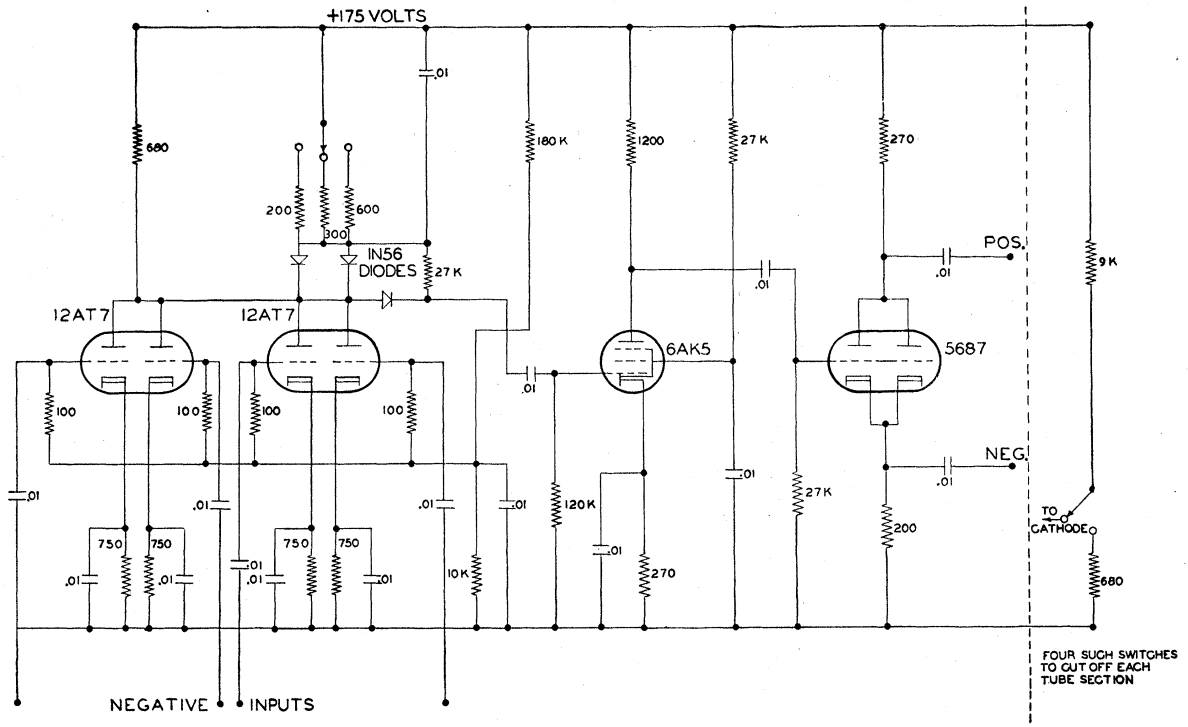

FIG. 4. Diagram of the coincidence circuits.

[5] R. L. Garwin, Rev. Sci. Instr. **21**, 569 (1950).

The meson pulses, as seen with the fast Tektronix Type 517 Oscilloscope, were quite uniform in amplitude.

The counting efficiency of these scintillators should be very close to 100 percent. An over-all check was obtained by comparing the quadruples to doubles rate with counters No. 3 and No. 4 between No. 1 and No. 2 in the line of the pion beam. The ratio obtained was usually quite close to unity.

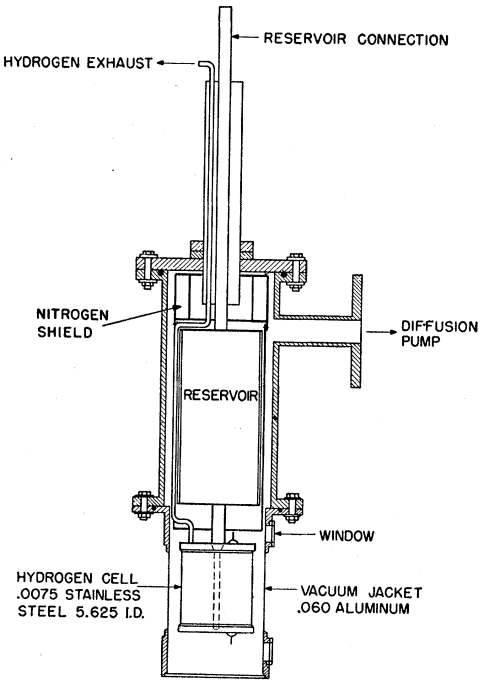

FIG. 5. Liquid hydrogen container.

III. TARGET

The beryllium target in which the mesons are produced has a calibrated thermocouple arrangement which records on a Brown potentiometer the power in watts delivered to the target by the proton beam. Most of this energy is due to ionization loss, some is due to nuclear reactions, but in any case the energy delivered is closely proportional to the path length of protons in the target and hence to the number of mesons produced.

The readings obtained from the thermocouple target do not enter in any essential way in the present experiments. However, by reducing the counting rate to unit energy in watt minutes developed in the target, an over-all check on the operation of the equipment is provided which is useful not only during a given run, but also in judging the reproducibility of the arrangement from one day's run to the next.

In the present experiments the beryllium target was of dimensions 2 in. in the direction of the beam, $\frac{1}{2}$ in. in height and $\frac{1}{4}$ in. in thickness. In most of the runs the intensity ranged from 10 to 25 watts. At the level of operation of 12 watts the double coincidences of counters No. 1 and No. 2 which register the pions entering the equipment were as follows: For positive pions of 78 Mev, 36 000 per minute; for positive pions of 110 Mev, 6000 per minute; for positive pions of 135 Mev, 900 per minute; for negative pions of 120 Mev, 230 000 per minute; and for negative pions of 144 Mev, 65 000 per minute.

IV. HYDROGEN CONTAINER

During the course of this investigation two different liquid hydrogen containers were used. They differed primarily in the materials and the thickness of the two walls of the liquid hydrogen Dewar. One was used in all measurements on positive pions and the other in the measurements of negative pions.

The apparatus for holding the liquid hydrogen is shown in Fig. 5. The mesons passed horizontally through the lower section, where the walls were thinned. In the cell used for the positive pion measurements the outer wall was 0.032-in. stainless steel and the inner wall 0.020-in. brass, and the internal diameter 5.8 in. For the measurements on negative pions, the outer wall was 0.060-in. aluminum and the inner wall 0.0075-in. stainless steel, internal diameter $5\frac{5}{8}$ in. The space between the walls was evacuated to a pressure of about 10^{-6} mm of mercury. The inner cylindrical cell which held the liquid hydrogen had a volume of about 4 liters. A reservoir of 12 liters capacity was directly above the cell and connected to it by a $\frac{3}{8}$-in. diameter tube extending nearly to the bottom of the cell. At the top of the cell there was an exhaust tube which carried off the vapors when liquid filled the cell. Whenever it was required to remove the liquid from the cell, the exhaust tube was closed externally by a valve: whereupon the vapor pressure forced the liquid up into the reservoir. Opening the exhaust valve allowed the liquid to fall back into the

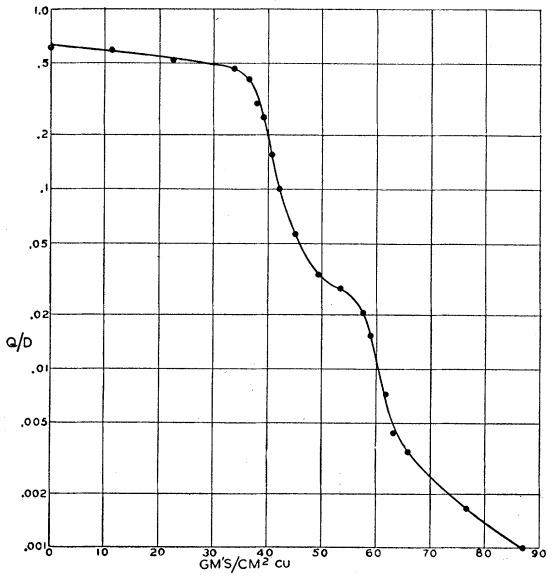

FIG. 6. Range curve of π^+ in copper.

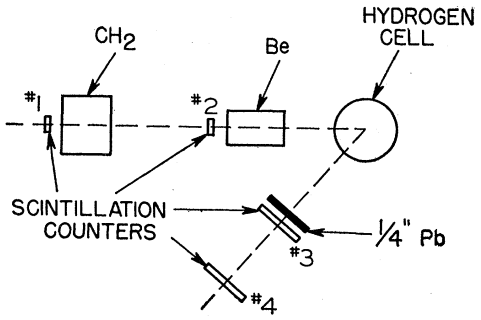

FIG. 7. Arrangement for Panofsky effect.

cell under gravity. By this method successive measurements of the pion scattering could be taken with the cell full or empty of liquid.

Two parallel plate condensers, one above and one below the cell, were used to indicate when the cell was full or empty of liquid, use being made of the sizeable increase in capacity which results when liquid hydrogen fills the space between the condenser plates.

The reservoir was shielded from radiation by a liquid nitrogen jacket so that the evaporation rate was about 0.6 liter per hour. With a 50-liter supply of liquid hydrogen it was possible to continue an experiment for about 24 hours.

V. ENERGY OF THE PRIMARY PIONS

The energy of the primary pions is known approximately from the channel through which they pass. These channels were laid out according to a rather detailed study of the trajectories of the pions of different energy. The channel energy is only nominal, however, because it depends on the target position and on the value of the cyclotron magnetic field, and these are not always precisely reproduced.

For this reason, it is more reliable to measure directly the energy of the pion beam used in each experiment. This has been done sometimes by taking a range curve of the pions and sometimes by observation of the Panofsky effect. A typical range curve is plotted logarithmically in Fig. 6. This was obtained with the positive pion beam from the channel of nominal energy 122 Mev. The four counters were put in line with no hydrogen in the scattering cell, and copper absorbers were inserted between counters No. 2 and No. 3. The absorption curve shows two sharp drops corresponding to the end of the range of the pions and of the muons. The uncorrected mean ranges from the curve are 38.4 and 59.8 g/cm² copper.

In order to compute the energy of the pions in the center of the liquid hydrogen, one must correct these ranges, on account of the different amount of absorbers present in the absorption measurement and in the scattering experiment. The range is finally converted to energy using the range energy tables for protons given by Aron[6] and adopting as a mass ratio 6.65 for the proton to pion. The range curve of Fig. 6 can also be used in order to estimate the contamination of the beam by muons and by electrons. For example, it was estimated that the muon contamination in this case was 7 percent.

In some of the experiments the beam energy was determined by means of the Panofsky effect. One of the geometries used for this type of measurement is shown in Fig. 7. A $\frac{1}{4}$-in. lead sheet was placed in front of counter No. 3 to increase its sensitivity to gamma-radiation. Light atomic weight absorbers, beryllium and

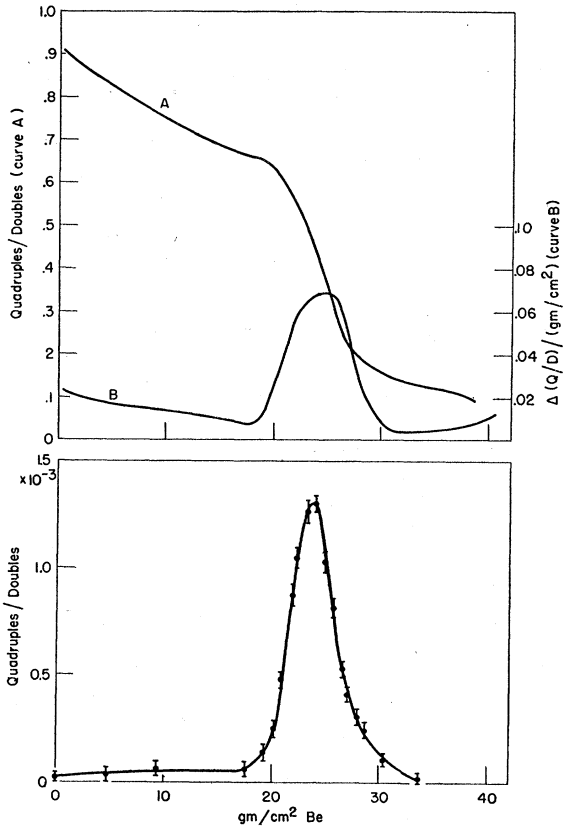

FIG. 8. Abscissas, amount of Be absorber; lower curve, intensity of the Panofsky gamma-radiation; upper curves, absorption curve and its derivative. The additional absorber of 11.24 g/cm² polyethylene between counters No. 1 and No. 2 is not indicated.

polyethylene, were interposed in the beam in front of the liquid hydrogen cell. In Fig. 8 the ratio of quadruple to double coincidences is plotted *versus* the thickness of absorber. The curve shows a sharp maximum at 23.8 g/cm² beryllium. To this one should add the absorber (11.24 g/cm² polyethylene) between counters No. 1 and No. 2. The beryllium equivalent of this is 14.6 g/cm². In conclusion the amount of beryllium necessary to reduce the energy of the pions to the point that they stop in the hydrogen is 38.4 g/cm², corresponding to an energy of 110 Mev.

[6] W. A. Aron, Berkeley Report UCRL 1325, 1951 (unpublished).

TABLE I. Observed value of $10^6 Q/D$ for 110 Mev and 135 Mev positive pions (4-in. diameter counters, corrected to standard geometry).

Angle	With hydrogen	Without hydrogen	Net
	110 Mev		
45°	262.6±15.0	162.3±18.4	100.4±19.8
90°	124.0±10.5	21.0± 6.7	103.0±12.5
135°	243.5±12.7	50.5± 8.1	193.0±15.1
	135 Mev		
45°	454±47	280±47	174±67
90°	199±32	63±28	136±43
135°	403±45	74±30	329±54

In the upper part of Fig. 8 there is plotted the absorption curve obtained in the same geometry of the Panofsky effect, and its derivative. One can see the maximum in the derivative curve matching the Panofsky maximum. A discussion of the quantitative comparison between the two curves will be found in Sec. VIII.

VI. SCATTERING OF POSITIVE PIONS

For positive pions only the elastic scattering, represented by

$$\pi^+ + p \rightarrow \pi^+ + p \qquad (1)$$

was considered possible. After the scattering, a pion and a proton are produced which share the kinetic energy of the primary pion. In our experiment the conditions were always such that the protons could not be detected because they did not have sufficient range to penetrate the detecting counters No. 3 and No. 4. For this reason all observed scattering was attributed to the scattered positive pions. Scattering measurements of positive pions have been performed at three energies of primary pions, 78 Mev, 110 Mev, and 135 Mev (mean energy at center of hydrogen). Measurements were taken for three scattering angles, 45°, 90°, and 135°. At each of these positions, counts were taken both with and without hydrogen in the scattering cell, and the difference of the two results attributed to the hydrogen scattering.

In the measurements at 110 Mev and 135 Mev the 4-in. diameter detecting counters were used in positions 3 and 4. In the 135-Mev measurement the distances of No. 3 and No. 4 from the center of the scattering cell were the "standard" distances 9 in. and 17 in. In some of the measurements at 110 Mev distances of 8.7 in. and 16.7 in. were used, in others the distances were 10.8 in. and 18.8 in. The data for this case are corrected to the "standard" geometry. One measures in both cases the ratio Q/D of quadruple to double coincidences. The results are given in Table I.

In order to compute from these data the corresponding scattering cross section for each angle, the effective solid angle subtended by counters No. 3 and No. 4 is needed. For the scattering angles 45° and 135°, this was 0.0435 steradian. For the 90° geometry, the effective solid angle was 0.0410 steradian, slightly less because some of the particles scattered at the entrance or at the exit of the scattering cell could enter counter No. 4, but not counter No. 3, and would be missed. In computing the cross sections, the fact that only 93 percent of the primary beam were pions was taken into account. The muons, and possibly some few electrons in the beam were assumed not to be scattered appreciably.

The mean path length of pions traversing the hydrogen in these experiments was 14.4 cm. When the cell was filled with liquid hydrogen, the number of atoms/cm^3 was 4.2×10^{22}. When the cell was empty, it still contained gaseous hydrogen at liquid hydrogen temperature amounting to 0.07×10^{22} atoms/cm^3. The difference, 4.13×10^{22}, multiplied by the effective length of the scattering cell, gives 5.95×10^{23} H atoms/cm^2.

The efficiency of counters No. 3 and No. 4 for counting a scattered pion that geometrically should be accepted by both counters was not 100 percent because the counter efficiency was not perfect (98 percent), and nuclear absorption in the first counter and in the hydrogen cell further reduced the efficiency to about 93 percent. The cross sections per steradian are given in Table II in the laboratory and in the center-of-mass systems.

TABLE II. Differential cross sections for positive pions.

Energy Mev	Laboratory system: Scattering angle (degrees)	Laboratory system: Differential cross section 10^{-27} cm^2/sterad	Center-of-mass system: Scattering angle (degrees)	Center-of-mass system: Differential cross section 10^{-27} cm^2/sterad
78	45°	1.96±0.33	53.8°	1.50±0.25
	90°	2.26±0.31	102.0°	2.34±0.32
	135°	3.09±0.34	143.2°	4.29±0.47
110	45°	4.48±0.88	54.9°	3.33±0.65
	90°	4.88±0.59	103.2°	5.09±0.62
	135°	8.62±0.67	143.9°	12.34±0.96
135	45°	7.77±3.00	55.7°	5.66±2.18
	90°	6.42±2.03	104.2°	6.75±2.14
	135°	14.70±2.41	144.5°	21.64±3.55

The probable errors given in Table II are those due to statistics alone. Uncertainties in the beam energy and its pion content as well as in the estimates of the efficiency of detection all contribute to the inaccuracy of the experiment. These additional errors have not been added in this case because the statistical error was believed to be dominant.

The measurement with 78-Mev positive pions was performed at a later date using as detecting counters No. 3 and No. 4 the rectangular 4 in.×6 in. counters. In this case the distances of the two counters No. 3 and No. 4 from the center of the scattering cell were respectively 9 in. and 17 in. The beam intensity at the average operation level of 23 watts yielded approximately 70 000 doubles per minute. The results of the measurement are collected in Table III. The conversion of these data to cross sections is similar to the previous cases. We assumed in this case that 92 percent of the doubles were due to pions. The solid angle was ap-

proximately 0.083 with very minor geometrical and scattering corrections. The cross sections in the laboratory and in the center-of-mass system are given in Table II. It will be noticed that in all these cases $(d\sigma/d\omega)$ is appreciably larger in the backward than in the forward direction. This fact seems to indicate a negative interference between the scattering due to the s and the p waves, as will be discussed later.

The differential cross sections in the laboratory system can be integrated over the solid angle in order to obtain the total cross sections. The results are given in column 2 of Table IV. In column 3 of the same table are reported the cross sections at the same energy obtained by interpolation from the data of the transmission measurements.[2] The agreement is within the experimental error.

TABLE III. Observed values of $10^6Q/D$, 78-Mev positive pions (4-in.×6-in. counters, standard geometry).

Angle	With hydrogen	Without hydrogen	Net
45°	510.9±10.4	425.7±9.8	85.2±14.3
90°	217.5±10.4	121.5±7.8	96.0±13.0
135°	390.9±11.4	256.6±9.3	134.4±14.8

VII. SCATTERING OF NEGATIVE PIONS

The measurement of the scattering of negative pions was carried out for two energies of the primary beam, 120 and 144 Mev (mean energy at the center of the hydrogen). Three processes are believed to be possible:

$$\pi^-+p\rightarrow\pi^-+p, \quad (2)$$

$$\pi^-+p\rightarrow\pi^0+n\rightarrow 2\gamma+n, \quad (3)$$

$$\pi^-+p\rightarrow\gamma+n. \quad (4)$$

TABLE IV. Total cross sections of positive pions.

Energy	Total cross section 10^{-27} cm² From integration	From transmission
78 Mev	31± 3	45±13
110 Mev	77± 6	82± 8
135 Mev	126±20	149±14

Equation (2) represents the elastic scattering of negative pions and protons. Equation (3) represents scattering with charge exchange, in which the proton is converted to a neutron and the negative pion is converted to a neutral pion which almost immediately disintegrates into two photons. Equation (4) is the inverse reaction of the photoeffect in which a photon produces a negative pion by striking a neutron. The cross section of process (4) is estimated by detailed balancing from the inverse process[7] to be only about 0.8×10^{-27} cm². The present measurements confirmed the fact, previously reported,[8] that process (3) is appreciably more intensive than process (2).

The sensitivity of the pair of counters No. 3 and No. 4 to photons produced in the scattering process is normally rather low. However, it can be increased very appreciably by interposing in front of counter No. 3 a lead sheet to convert the gamma-rays into electron-positron pairs which are detected by the counters. For this reason, with π^-, four measurements were taken at each angle, namely, measurements of the ratio Q/D with and without liquid hydrogen in the scattering chamber and with and without a $\frac{1}{4}$-in. thick lead radiator in front of counter No. 3. The net effect due to the hydrogen is computed as the difference with and without hydrogen.

In order to obtain separately the numbers of scattered pions and photons entering the detecting counters No. 3 and No. 4 it is necessary to know the efficiencies for the two types of particles. The counters used in the experiments on negative pions were thinner than those used in the positive pion experiments. There was a smaller loss due to absorption. The over-all efficiency without lead radiator was estimated to be 97 percent. With the lead radiator the efficiency is reduced both by nuclear absorption and by scattering. The latter effect depends on the energy of the pions and therefore also on the scattering angle. Moreover, the geometry at 90° is somewhat different than at 45° and 135°. An estimate of these effects gives the efficiencies listed in Table V.

In the same table the efficiencies for photon detection with and without lead are listed. The procedure for calculating these efficiencies is described in Sec. VIII.

The energies of the primary negative pions used in these two measurements were determined from the amount of absorber needed to produce a maximum in the Panofsky radiation. In one set of measurements the absorber was 44.3 g/cm² of aluminum corresponding to a pion energy of 120 Mev. In the other measurements it was 57.3 g/cm² of aluminum corresponding to 144 Mev. In both cases the detecting counters No. 3 and No. 4 had a sensitive area of 4×6 sq in., and were placed re-

TABLE V. Efficiencies of the detecting counters.

Energy Mev	Angle	Lead	Efficiency for pions (percent)	Efficiency for photons (percent)
120	45°	out	97	4
120	45°	in	91	67
120	90°	out	97	4
120	90°	in	88	61
120	135°	out	97	4
120	135°	in	88	59
135	45°	out	97	4
135	45°	in	92	70
135	90°	out	97	4
135	90°	in	89	63
135	135°	out	97	4
135	135°	in	88	60

[7] Bishop, Steinberger, and Cook, Phys. Rev. **80**, 291 (1950); Feld, Frisch, Lebow, Osborne, and Clark, Phys. Rev. **85**, 680 (1952).

[8] Fermi, Anderson, Lundby, Nagle, and Yodh, Phys. Rev. **85**, 935 (1952).

spectively, at 9 in. and 17 in. from the center of the scattering cell.

Each individual measurement consists of a determination of the ratio Q/D of the quadruple coincidences to the double coincidences. The results of the measurements with their statistical errors are collected in Table VI.

For each primary energy and for each scattering angle, one needs the numbers Π and Γ of pions and photons per million primaries whose line of propagation enters the solid angle subtended by counter No. 4. These two numbers are obtained by solving two linear equations. For example, for 120-Mev pions and 90° scattering angle, we have from Table VI counts per million with and without lead 103.4 ± 4.0 and 25.6 ± 3.2. Using the efficiencies listed in Table V, one obtains the two equations

$$0.61\Gamma+0.88\Pi=103.4\pm4.0,$$
$$0.04\Gamma+0.97\Pi=25.6\pm3.2.$$

These equations have the solution

$$\Gamma=139.8\pm8.7, \quad \Pi=20.6\pm3.6.$$

In order to convert these numbers to differential cross sections they must be divided by the following factors: 930 000 (this is the number of pions per million primaries, the remainder of 7 percent being due to muons and electrons which are assumed to have no appreciable nuclear scattering), 0.083 (this is the solid angle subtended by counter No. 4), 5.9×10^{23} (this is the average number of hydrogen atoms per cm² traversed by the primary beam). Dividing the values of Π and Γ by the product of these factors, one obtains the following cross sections per steradian at 90°, for 120-Mev negative pions:

$$d\sigma_-/d\omega=(0.45\pm0.08)\times10^{-27}\ \text{cm}^2/\text{sterad},$$

and

$$d\sigma_\gamma/d\omega=(3.08\pm0.20)\times10^{-27}\ \text{cm}^2/\text{sterad}.$$

The errors indicated in these two cross sections comprise only the statistical error. Other sources of error are, in order of importance, the uncertainty in the efficiencies listed in Table V in the actual pion content and energy of the beam, and geometrical errors. We have estimated that the over-all effect of these errors may amount to 10 percent, and this error has been combined with the statistical error in the final results.

In Table VII are collected the values of the differential cross sections in the laboratory and in the center-of-mass frames of reference.

As an over-all check the total cross sections obtained by integration from the data of Table VII may be compared with the results of total cross-section measurements by transmission.[1] The results of the integration are collected in Table VIII, columns 2 and 3. The contribution of the $\pi^-\to\gamma$ process to the total cross section is about one-half the cross section listed in column three because each neutral pion produced in the exchange scattering process yields two photons. A very small correction has been included on account of the contribution of the inverse photoeffect. The total cross section obtained from the contributions of columns 2 and 3 is given in column 4. The total cross section given in column 5 is obtained instead by interpolation of the results of the transmission measurements. The two sets of results agree within the experimental errors.

TABLE VI. Observed values of $(Q/D)\times10^6$ for negative pions.

Angle	Lead	With hydrogen	Without hydrogen	Net
		120 Mev		
45°	out	235.6±3.3	167.2±2.8	68.4±4.5
90°	out	82.0±2.3	56.4±2.1	25.6±3.2
135°	out	112.7±2.8	75.1±3.1	37.6±4.2
45°	in	290.6±4.3	150.4±3.4	140.2±5.6
90°	in	161.4±3.2	58.0±2.4	103.4±4.0
135°	in	223.9±3.9	75.8±3.1	148.1±5.0
		144 Mev		
45°	out	237.6±4.9	126.0±4.0	111.6±6.4
90°	out	93.3±3.4	55.0±3.0	38.3±4.6
135°	out	135.3±3.9	88.5±4.2	46.8±5.8
45°	in	355.9±6.0	115.1±1.8	240.8±7.1
90°	in	202.2±5.0	52.3±3.0	149.9±5.9
135°	in	264.1±5.2	75.3±4.3	188.8±6.8

TABLE VII. Differential cross sections for negative pions.

Energy (Mev)	Process	Laboratory system: Scattering angle (degrees)	Laboratory system: Diff. cross section (10^{-27} cm²/sterad)	Center-of-mass system: Scattering angle (degrees)	Center-of-mass system: Diff. cross section (10^{-27} cm²/sterad)
120	$\pi^-\to\pi^-$	45	1.44±0.18	55.2	1.06±0.14
		90	0.45±0.09	103.6	0.47±0.10
		35	0.67±0.12	144.3	0.97±0.18
120	$\pi^-\to\gamma$	45	2.64±0.36	53.0	2.07±0.30
		90	3.08±0.37	100.5	3.19±0.39
		135	4.53±0.51	142.0	5.98±0.69
144	$\pi^-\to\pi^-$	45	2.35±0.29	56.0	1.70±0.21
		90	0.69±0.14	104.6	0.73±0.15
		135	0.83±0.17	144.6	1.23±0.25
144	$\pi^-\to\gamma$	45	4.48±0.55	54.0	3.43±0.42
		90	4.25±0.51	101.6	4.43±0.53
		135	5.71±0.66	142.6	7.78±0.90

VIII. SENSITIVITY OF THE DETECTING COUNTERS FOR PHOTONS

The sensitivity of the detecting counters No. 3 and No. 4 for the photons produced in the decay of neutral pions is very small without lead radiator and is of the order of magnitude of 50 percent with the lead radiator in place. Without the lead radiator a photon may be detected when it materializes while traversing the hydrogen, the wall of the hydrogen cell, or counter No. 3, provided in this latter case that the materialization does not take place too close to the exit of the photon out of the sensitive region of the counter because the

pulse will then be too small to be recorded. Finally, according to Dalitz,[9] a photon has a probability of 0.63 percent of being converted into a pair by internal conversion at the moment of its formation. In order to compute these various effects, the cross section for pair formation was obtained by interpolation between the data of Lawson[10] at 88 Mev and the data of DeWire, Ashkin, and Beach[11] at 280 Mev. Some small contribution to the detection of gamma-rays comes from Compton electrons. A Compton electron, however, has a high probability to give a coincidence of counters No. 3 and No. 4 only when its energy is an appreciable fraction of the energy of the photon. For this reason only one-half of the Compton cross section was added to the pair formation cross section, in order to obtain an effective cross section for materialization. The cross sections finally adopted are given in Table IX.

TABLE VIII. Integrated cross sections of negative pions (10^{-27} cm^2).

Energy	$\pi^-\to\pi^-$	$\pi^-\to\gamma$	Total	Total from transmission
120 Mev	11.3±1.6	43.4±5.4	33.4±3.2	38±9
144 Mev	17.0±2.4	61.2±7.5	48.1±4.5	55±6

TABLE IX. Cross sections for materialization σ pair$+\frac{1}{2}\sigma$ Compton (cm^2/g).

Element	90 Mev	135 Mev
H	0.0097	0.0097
C	0.0135	0.0143
Al	0.0240	0.0256
Fe	0.0422	0.0453
Cu	0.0454	0.0487
Pb	0.0909	0.0983

The probability of observing a photon without the lead radiator computed for the average energy photon emerging in the various directions and for the actual thickness of material traversed was in all cases about 4 percent, and this value has been adopted in Table V. With the lead radiator in place (7.36 g/cm^2), the probability of pair formation is greatly increased. For example, for 90-Mev photons, it is 51 percent.

The probability of pair formation, however, gives only a rough indication of the efficiency. There are primarily two reasons for this, namely, absorption of the electrons and effect of the multiple scattering. The first effect leads to a reduction, the second to an increase in efficiency. In order to understand the reason for the increase, we observe that if a single particle and not a pair were produced in the materialization, the effect of the multiple scattering would be cancelled in first approximation because some particles would be scattered in and some would be scattered out. In the case of a pair, however, it is sufficient that one electron only of the pair be detected; therefore a photon is lost if both electrons are scattered out but is detected if both electrons or even only one of them is scattered in. An attempt was made to calculate these effects by assuming that all the pairs originate in the middle of the lead radiator. It was assumed further that the energy of the photon is divided evenly between the electron and the positron. The calculation was carried out for photons of 90 and 135 Mev. From the results of Wilson[12] it was estimated that the probability of a pair electron traversing the lead with sufficient energy to be recorded is 0.76 for photons of 90 Mev and 0.85 for photons of 135 Mev.

TABLE X. Efficiency for photons.

Angle of scattering	90 Mev	135 Mev
45° or 135°	0.567	0.691
90°	0.558	0.681

TABLE XI. Mean energy of the photons (Mev).

Primary pions \ Angle	45°	90°	135°
120 Mev	126	109	97
144 Mev	137	117	102

Consider now a photon whose line of propagation crosses the plane of counter No. 4 at a certain position. If a pair is formed, the probability q of observing the positron of the pair will be obtained by multiplying the probability that the positron of the pair escapes the lead with sufficient energy to be counted times the probability that after multiple scattering the positron falls inside counter No. 4. There is, similarly, an equal probability q of observing the electron of the pair. The probability of observing the photon that has materialized is the probability of observing either the electron or the positron or both. This probability is given by $q(2-q)$. Multiplying this probability by the probability of materialization of the photon, one obtains the probability of observing the photon. Integrating this probability over the area, one obtains an effective area of counter No. 4. We define the efficiency as the ratio of the effective to the true area of the counter. The geometry is slightly different at 90° and at 45° and 135°. The computed efficiencies are given in Table X. It is seen that the efficiency has an appreciable energy dependence. The mean energy of the photons produced by neutral pion decay in the scattering experiment depends on the energy of the primaries and the scattering angle as is given in Table XI. The efficiencies were then

[9] R. H. Dalitz, Proc. Roy. Soc. (London) **A64**, 667 (1951).
[10] J. L. Lawson, Phys. Rev. **75**, 433 (1949).
[11] DeWire, Ashkin, and Beach, Phys. Rev. **83**, 505 (1951).
[12] R. R. Wilson, Phys. Rev. **84**, 100 (1951).

computed by linear interpolation from the data of Table X and are given in Table V.

An attempt was made to obtain an experimental confirmation of the results of the efficiency calculation described in this section. This is done by an absolute measurement of the sensitivity of the detecting counters No. 3 and No. 4 to the gamma-rays emitted in the Panofsky effect. In Fig. 8 the ratio of quadruple to double coincidences is plotted *versus* the thicknesses of absorber for the geometry represented in Fig. 7. By integration of the curve of Fig. 8 one finds that the total area of the Panofsky bulge after subtracting background is

$$P=6430 \text{ counts per million} \times \text{g/cm}^2 \text{ Be}.$$

In the same figure is plotted also the derivative of the absorption curve. The derivative curve shows a bulge matching in position the Panofsky bulge. Its integrated area after subtracting background is found to be

$$A=4.41\times10^5 \text{ counts per million}.$$

The thickness of hydrogen traversed by the pions is in the average 0.987 g/cm². Using for short range pions the equivalence factor in stopping power of hydrogen to beryllium of 2.58 one finds that this amount of hydrogen is equivalent to 2.546 g/cm² Be. Denoting this factor by H, we obtain now the effective solid angle ω of the detecting counters from the following relationship:

$$P=fHA\omega/4\pi,$$

where f is the average number of photons emitted when a negative pion comes to rest within the liquid hydrogen. According to Panofsky[13] one has $f=1.485\pm0.054$. We obtain in this way $\omega=0.0485\pm0.005$. The error includes an estimate of the uncertainties in the various quanties that enter in the determination of ω. The efficiency is the ratio of the effective solid angle ω to the geometrical solid angle which is 0.083. We obtain, therefore, an efficiency of 0.58 ± 0.06. The average energy of the pions to which this result refers is about 90 Mev. In Table X the efficiency was found, in excellent agreement, to be 0.57.

IX. ANALYSIS OF THE SCATTERING DATA

The data of Secs. 6 and 7 may be analyzed by assuming that the scattering is due mainly to the contributions of s and p waves. The angular distribution of the scattered particles in the center-of-mass system will then have the form

$$d\sigma/d\omega=a+b\cos\chi+c\cos^2\chi, \tag{5}$$

where χ is the scattering angle in the center-of-mass system. The coefficients a, b, and c for the elastic scattering of 78, 110, and 135 Mev π^+ and for the elastic scattering of 120 and 144 Mev π^- are readily computed from the data of Tables II and VII.

[13] Panofsky, Aamodt, and Hadley, Phys. Rev. **81**, 565 (1951).

The calculation of these coefficients for the charge exchange scattering is complicated by the fact that the direct measurement gives the cross section for the production of gamma-rays, and the angular distribution of these differs somewhat from that of the neutral pions which decay into them.

The problem can be solved by imagining the angular distribution of the neutral pions in the center-of-mass system to be analyzed into spherical harmonics. Each spherical harmonic component in the original distribution of the neutral pions gives rise, in the gamma-ray distribution, to a component proportional to the same spherical harmonic multiplied by a constant coefficient. The value of this coefficient depends upon the order of the spherical harmonic in question. It is equal to 2 for spherical harmonics of the order zero; to

$$k_1=\frac{2\gamma}{\eta}-\frac{1}{\eta^2}\ln\frac{\gamma+\eta}{\gamma-\eta} \tag{6}$$

TABLE XII. Coefficients of $d\sigma/d\omega=a+b\cos\chi+c\cos^2\chi$ for various processes (10^{-27} cm²/sterad).

Energy Mev	λ (10^{-13} cm)	Process	a	b	c
53	1.777	$+\rightarrow+$	0.46±0.39	−0.08±0.84	3.60±1.46
78	1.439	$+\rightarrow+$	1.9 ±0.3	−1.7 ±0.4	1.6 ±0.9
110	1.186	$+\rightarrow+$	3.6 ±0.7	−4.8 ±0.8	7.5 ±1.9
135	1.057	$+\rightarrow+$	3.9 ±2.3	−7.1 ±2.8	18.0 ±6.8
120	1.129	$-\rightarrow-$	0.49±0.11	0.34±0.16	1.16±0.34
144	1.018	$-\rightarrow-$	0.82±0.16	0.73±0.24	1.52±0.50
120	1.129	$-\rightarrow\gamma$	2.68±0.40	−2.39±0.46	2.29±1.20
144	1.018	$-\rightarrow\gamma$	3.80±0.55	−2.49±0.62	3.17±1.62
120	1.129	$-\rightarrow0$	0.6 ±0.4	−1.9 ±0.5	3.2 ±1.7
144	1.018	$-\rightarrow0$	1.05±0.5	−1.9 ±0.5	3.9 ±2.0

for spherical harmonics of order one; and to

$$k_2=2+\frac{6}{\eta^2}-\frac{3\gamma}{\eta^3}\ln\frac{\gamma+\eta}{\gamma-\eta} \tag{7}$$

for spherical harmonics of order two. In the above equations η and γ are the momentum and the total energy of the neutral pion in the center-of-mass system, in units of μ_0c and μ_0c^2, respectively.

Writing (5) for neutral pions as the sum of spherical harmonics

$$a+\tfrac{1}{3}c+b\cos\chi+c(\cos^2\chi-\tfrac{1}{3}), \tag{8}$$

and applying the above coefficients, the angular distribution for the π^0 gamma-rays in the center-of-mass system is found to be

$$d\sigma_\gamma/d\omega=2a+\tfrac{1}{3}(2-k_2)c+k_1b\cos\chi+k_2c\cos^2\chi. \tag{9}$$

It is seen that the gamma-rays originating from the π^0 decay also have an angular distribution of the type (5) and one can readily compute the coefficients for the angular distribution of the neutral pions from the measured coefficients for the angular distribution of the photons.

Table XII summarizes the values of the coefficients a, b, and c for all the reactions studied. The first column gives the energy of the primary beam in Mev, the second column gives the deBroglie wavelength divided by 2π, in the center-of-mass system. The third column indicates the type of reaction; 0, +, and − are used to indicate neutral, positive, and negative pions, γ for the photons. The next three columns are the coefficients a, b, and c for the reaction in question. The data at 53 Mev are computed from cross-sections measured at Brookhaven with a diffusion cloud chamber.[14]

Striking features of the table are the rather large values of the coefficients b and c which indicate strong deviations from spherical symmetry. The negative values of b for $\pi^+\rightarrow\pi^+$ and $\pi^-\rightarrow\pi^0$ corresponds to the predominance of the backward scattering of these processes. The coefficient b has a positive value for $\pi^-\rightarrow\pi^-$ because, in this case, by contrast, the scattering is more pronounced in the forward direction.

X. PHASE SHIFT ANALYSIS

The data may be analyzed on the assumption that in the scattering of pions by nucleons the isotopic spin is conserved, or more precisely, that the isotopic spin behaves as a quantized angular momentum vector in isotopic spin space.[15] In the scattering of positive pions by protons only the isotopic spin $\frac{3}{2}$ will be involved because both the proton and the pion have their isotopic spin vectors "up." In the scattering of negative pions by protons, on the other hand, the orientation of the vectors is mixed and both isotopic spins, $\frac{3}{2}$ and $\frac{1}{2}$, will be involved.

From this basic assumption, it follows that the scattering features at any given energy will be determined by the phase shifts of the different states of given isotopic spin, orbital and total angular momentum. If it is assumed, as was done in the previous section, that only s- and p-states are important, there will be six phase shifts at each energy. They correspond to the possible values $\frac{3}{2}$ and $\frac{1}{2}$ of the isotopic spin, and, for each isotopic spin value, to the s-wave shifts and to the phase shifts of the two p-waves of angular momenta $\frac{3}{2}$ and $\frac{1}{2}$.

A complete set of measurements at any given energy consists of nine data: the values of the differential cross sections for each of the three processes $\pi^+\rightarrow\pi^+$, $\pi^-\rightarrow\pi^0$, and $\pi^-\rightarrow\pi^-$, at each of three angles. Alternately the experiments supply nine constants, a, b, and c for each of the three reactions observed. If the assumptions are correct, these nine data will be expressible in terms of the six phase shifts, a situation which permits a check of the soundness of the procedure.

To obtain a complete set of data at each of two energies we have interpolated the π^+ data obtained at 110 Mev and 135 Mev to give values at 120 Mev to go with the π^- data at this energy. We interpolated the π^- data between 120 Mev and 144 Mev to give values at 135 Mev to go with the π^+ data at this energy. The measurements at 78 Mev, on the other hand, are incomplete because only the π^+ reaction was investigated. However, in this case, only the three phase shifts for isotopic spin $\frac{3}{2}$ are involved. The data allow these phase shifts to be calculated but nothing remains for an internal check.

The phase shifts of the s waves of isotopic spin $\frac{3}{2}$ and $\frac{1}{2}$ will be indicated by α_3 and α_1. The phase shifts of the p waves will be indicated by α_{33}, α_{31}, α_{13}, α_{11}, where the first index is twice the isotopic spin of the state in question and the second index is twice the angular momentum. The quantities a, b, and c for the reaction $\pi^+\rightarrow\pi^+$ will be indicated by a_+, b_+, c_+. Similarly they will be indicated by a_-, b_-, c_-, for the reaction of elastic scattering of the negative pions, and by a_0, b_0, c_0 for the exchange scattering of the negative pions. In order to express the nine quantities a, b, c in terms of the six angles α, it is convenient to introduce the following notation:

$$e_3=e^{2i\alpha_3}-1,\ \cdots,\ e_{11}=e^{2i\alpha_{11}}-1. \tag{10}$$

By applying the standard procedures of the phase shift analysis of the collision theory, the amplitudes of the scattered waves may be expressed in terms of these quantities. There are nine such amplitudes in all. Three corresponding to the scattering of positive pions; amplitude of the scattered s wave and amplitudes of the scattered p waves with and without spin flip. These are indicated by B, A_β, and A_α. The scattering of the negative pions contributes six amplitudes because in each case scattering without and with exchange of charge must be considered. The corresponding amplitudes are indicated by B_p, $A_{p\beta}$, and $A_{p\alpha}$ for the non-exchange process, and B_n, $A_{n\beta}$, and $A_{n\alpha}$ for the exchange process. These nine scattering amplitudes are given in terms of the quantities e of (10) by the relations

$$\begin{aligned}
&B=e_3;\quad A_\beta=\tfrac{1}{3}\sqrt{2}(e_{33}-e_{31});\quad A_\alpha=\tfrac{1}{3}(2e_{33}+e_{31});\\
&B_p=\tfrac{1}{3}(e_3+2e_1);\quad A_{p\beta}=(\sqrt{2}/9)(e_{33}-e_{31}+2e_{13}-2e_{11});\\
&\qquad\qquad A_{p\alpha}=(1/9)(2e_{33}+e_{31}+4e_{13}+2e_{11});\\
&B_n=\tfrac{1}{3}\sqrt{2}(e_3-e_1);\quad A_{n\beta}=(2/9)(e_{33}-e_{31}-e_{13}+e_{11});\\
&\qquad\qquad A_{n\alpha}=(\sqrt{2}/9)(2e_{33}+e_{31}-2e_{13}-e_{11}).
\end{aligned} \tag{11}$$

The coefficients a_+, b_+, c_+ for the scattering of positive pions are given by

$$\begin{aligned}
&\frac{a_+}{\lambda^2}=\frac{1}{4}|B|^2+\frac{9}{8}|A_\beta|^2;\quad \frac{b_+}{\lambda^2}=\frac{3}{4}(BA_\alpha^*+B^*A_\alpha);\\
&\qquad\qquad \frac{c_+}{\lambda^2}=\frac{9}{4}|A_\alpha|^2-\frac{9}{8}|A_\beta|^2.
\end{aligned} \tag{12}$$

In these formulas a star means complex conjugation. The quantities a_-, b_-, c_- and a_0, b_0, c_0 are given by

[14] Fowler, Fowler, Shutt, Thorndyke, and Whittemore, Phys. Rev. **86**, 1053 (1952).

[15] N. Kemmer, Proc. Cambridge Phil. Soc. **34**, 354 (1938); W. Heitler, Proc. Roy. Irish Acad. **51**, 33 (1946).

TABLE XIII. Cross sections computed from phase shifts at 120 Mev (10^{-27} cm²/sterad).

Process	Measured cross sections	Computed First solution	Computed Yang solution
$-\rightarrow-$	1.06±0.14	1.06	1.06
	0.47±0.10	0.48	0.47
	0.97±0.18	1.02	1.02
$+\rightarrow+$	4.26±1.16	4.15	4.12
	5.75±1.16	5.13	5.14
	16.00±1.82	15.15	15.09
$-\rightarrow\gamma$	2.07±0.30	2.06	2.07
	3.19±0.39	3.38	3.40
	5.98±0.69	6.01	6.00

Phase shifts

First solution:
$\alpha_3=-15.2°$; $\alpha_1=9.0°$; $\alpha_{33}=29.6°$; $\alpha_{31}=3.9°$; $\alpha_{13}=1.8°$; $\alpha_{11}=-2.8°$.
Yang solution:
$\alpha_3=-15.4°$; $\alpha_1=9.1°$; $\alpha_{33}=12.9°$; $\alpha_{31}=38.6°$; $\alpha_{13}=-1.4°$; $\alpha_{11}=3.8°$.

similar formulas in which B, A_β, and A_α are replaced, respectively, by B_p, $A_{p\beta}$, $A_{p\alpha}$ and B_n, $A_{n\beta}$, $A_{n\alpha}$. It is possible, of course, to eliminate the intermediary quantities e, B, A from (10), (11), and (12), and to express directly the nine quantities a, b, c in terms of the six angles α. The formulas, however, are more complicated and not as well suited to numerical calculations.

If the accuracy of our measurement of the nine cross sections at a given energy were high enough, it would be possible to use six of them for determining the six angles α. Then, if the basic assumptions were right, the remaining three cross sections would be given correctly in terms of the same angles. Since, however, the experimental errors are rather large, this procedure is not very effective and it is more fruitful to try to use all the available experimental information in determining for each energy the best set of angles α by a least squares method. Some attempts to obtain by this method a set of "best" phase shifts were made by numerical computation on a preliminary set of cross-section values already published.[3]

The problem of determining the best set of phase shifts at each energy is managed much more efficiently with a modern electronic computer.[16] We are indebted to Dr. N. Metropolis for carrying out these computations for us using the Los Alamos Maniac computer. Given a set of nine measured cross sections, with the experimental errors, the machine finds the best set of six phase shifts according to the least squares criterion. Such a solution minimizes a least square sum $M=\Sigma_1^9(\Delta_i/\epsilon_i)^2$, where ϵ_i is the experimental error in the ith cross section, and Δ_i is the deviation of the calculated from the observed cross section.

This procedure does not permit a determination of the sign of the phase shifts. One recognizes easily that if the sign of all the phase shifts is changed the cross sections are not affected. It would be possible in principle to determine the signs by a study of the interference of the nuclear scattering with the Coulomb scattering. Thus far, however, measurements of the scattering at angles sufficiently close to the forward direction to observe this interference have not been carried out. Aside from this indeterminacy of the sign, one might raise the question whether the determination of phase shifts is unique. It appears that there are two fairly equivalent sets of angles that yield a rather low value of the least square sum. One of them corresponds to angles fairly close to those already published[3] and will be called "first solution." Yang has pointed out[17] that there is a second solution, that, although not equivalent to the

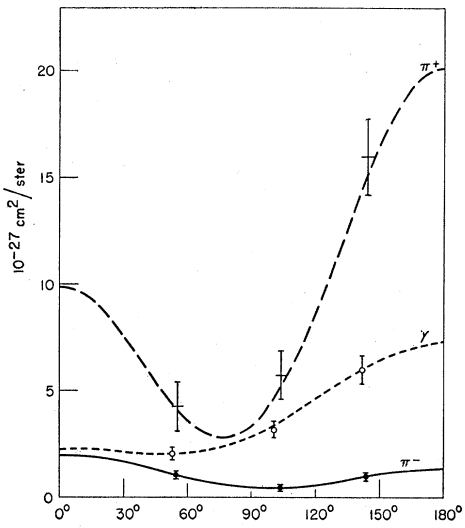

FIG. 9. Computed and observed cross sections at 120 Mev.

TABLE XIV. Cross sections computed from phase shifts at 135 Mev (10^{-27} cm²/sterad).

Process	Measured cross sections	Computed First solution	Computed Yang solution
$-\rightarrow-$	1.46±0.19	1.45	1.45
	0.63±0.13	0.63	0.63
	1.13±0.23	1.20	1.21
$+\rightarrow+$	5.66±2.18	6.35	6.20
	6.75±2.14	5.95	5.90
	21.64±3.55	18.13	17.95
$-\rightarrow\gamma$	2.92±0.38	2.85	2.85
	3.96±0.47	4.07	4.11
	7.10±0.82	7.40	7.36

Phase shifts

First solution:
$\alpha_3=-14.0°$; $\alpha_1=10.3°$; $\alpha_{33}=37.9°$; $\alpha_{31}=5.4°$; $\alpha_{13}=2.0°$; $\alpha_{11}=-4.6°$.
Yang solution:
$\alpha_3=-14.2°$; $\alpha_1=10.4°$; $\alpha_{33}=17.2°$; $\alpha_{31}=49.3°$; $\alpha_{13}=-2.9°$; $\alpha_{11}=5.6°$.

[16] E. Fermi and N. Metropolis, Los Alamos unclassified report LA-1492, 1952 (unpublished).
[17] C. N. Yang, private communication.

first, is in many cases almost eqully good. An extensive numerical analysis of the problem[16] has indicated that the first solution and the Yang solution are very probably the only two for which the least square sum is small. There is apparently another set of angles that yields a relative minimum of M. This, however, is so high as to make it of no practical value.

In Tables XIII and XIV are collected the cross sections for 120 Mev and for 135 Mev, together with the cross sections computed from the best sets of phase shifts. Results corresponding to the first solution and to the Yang solution are given. The agreement with the experimental results is extremely close for both solutions. Only a very considerable improvement in the experimental accuracy would permit to distinguish between the two.

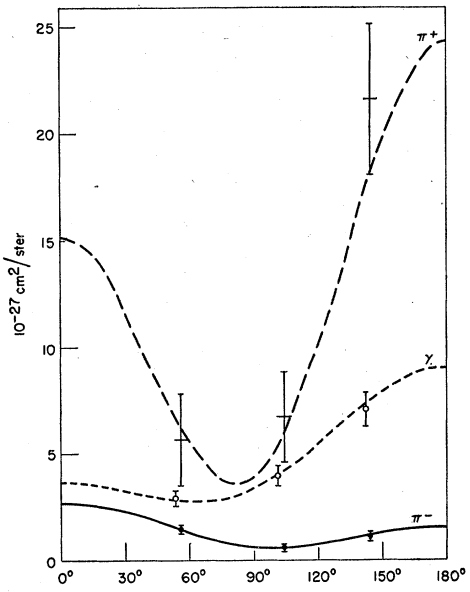

FIG. 10. Computed and observed cross sections at 135 Mev.

In Figs. 9 and 10 are plotted the cross sections in the center-of-mass system *versus* the scattering angle χ. The curves are computed from the scattering angles of the first solution. Also the experimental points are put on the same graph for reference.

TABLE XV. Phase shift angles.

		Phase shifts in degrees					
Mev	η	3	1	33	31	13	11
53	0.78	0		9	2		
78	0.97	−6		13	−3		
120	1.24	−15	9	30	4	2	−3
135	1.32	−14	10	38	5	2	−5

As pointed out above, the sign of all the phase shifts could be changed without affecting the cross sections. The sign chosen corresponds to the assumption that the interaction of the state with both isotopic spin and angular momentum equal to $\frac{3}{2}$ is attractive. Some arguments in favor of this assumption have been advanced by Peaslee[18] on the basis of an analysis of the scattering of negative pions by carbon.

At 78 Mev only the scattering of positive pions has been measured and consequently only three of the phase shifts could be determined. They are $\alpha_3=-6°$, $\alpha_{33}=13°$, $\alpha_{31}=-3°$. Also a similar analysis can be made on the data for scattering of 53-Mev positive pions by hydrogen published by the Brookhaven group.[14] The result is $\alpha_3=0°$, $\alpha_{33}=9°$, $\alpha_{31}=2°$. In Table XV are collected the various values of the phase shifts (first solution only). The second column gives the pion momentum in the center-of-mass system in units of μc. Due to experimental errors the phase shifts given above have an uncertainty of perhaps 5°. Experience gathered in successive calculations of the phase shifts has indicated, however, that some of them appear to be not very sensitive to changes in the cross sections, whereas others have a higher sensitivity and are for this reason less reliable. This appears to be particularly true of the phase shifts α_{13} and α_{11}.

XI. CONCLUSIONS

1. The fact that 9 cross sections measured at each energy can be represented in terms of 6 phase shifts is a demonstration of the fruitfulness of regarding the isotopic spin as a good quantum number. Such a demonstration would be even more meaningful if the experimental errors were smaller.

2. According to quantum mechanics one might expect that the phase shifts at sufficiently low energy should be

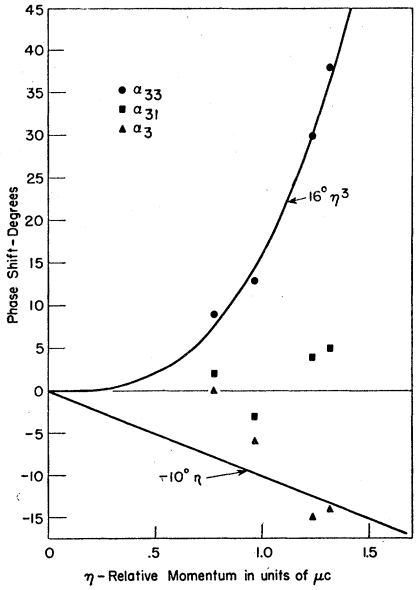

FIG. 11. Phase shifts plotted *versus* relative momentum.

[18] Quoted by H. Bethe at the Rochester Conference, December, 1952. See also G. F. Chew, Phys. Rev. **89**, 591 (1953).

proportional to the relative momentum η of the 2 colliding particles for s-terms and to η^3 for p-terms. In Fig. 11 some of the data of Table XV are plotted. The values of η are on the abscissas and the phase shifts of isotopic spin $\frac{3}{2}$ are plotted on the ordinates. One might expect that the phase shift α_3 should lie on a straight line through the origin. Actually the points do not at all show this property and this may or may not be due to the rather large experimental error. If one attempts to draw the "best" straight line through these points the coefficient of η would be approximately $-10°$. On the other hand, the points suggest an appreciably stronger dependence of α_3 on the energy. This in fact would be quite compatible with the possibility that α_3 may actually change sign at about 60 Mev, a possibility whose implications have been discussed by Marshak.[19] The ratio α_3/η at low energy gives the scattering length in units $\hbar/\mu c$. A coefficient of $-10°$ would correspond to a scattering length $a_3=-0.24\times10^{-13}$. However, this value for the reasons explained is quite tentative and even its sign could be wrong. Similarly from the data of Table XV we may make an equally tentative guess that the scattering length of the s-state of isotopic spin $\frac{1}{2}$ may be 0.18×10^{-13} cm.

The phase shifts α_{33} fit fairly well a proportionality to η^3 with a coefficient of about 16°. Very little can be said of the energy dependence of the other phase shifts α_{31}, α_{13}, and α_{11} which are so small that even their sign relative to that of the other phase shifts is uncertain with our present experimental accuracy.

3. We have already commented on the difficulties of deciding experimentally with our present accuracy between the phase shifts corresponding to the first solution and to the Yang solution of the problem. The previous conclusions are obtained on the assumption that the first solution is correct and would have to be modified appreciably if the Yang solution ultimately would turn out to be the right one. Similarly the over-all sign of the phase shifts is uncertain, and the opposite sign to the one chosen here may well be correct.

4. One might attempt to interpret phenomenologically the scattering as if it were due to a force acting between the nucleon and pion. Inspection of the variety of phase shifts obtained indicates immediately that this force should be quite different for different states. Assuming again the first solution to be correct, one would further conclude that the force is very large for the state of isotopic spin $\frac{3}{2}$ and angular momentum $\frac{3}{2}$. One can recognize that the same potential produces a much larger phase shift in the s terms than it does in the p-terms. For example, phase shifts of the order of magnitude observed could be attributed to a potential of radius $\hbar/\mu c$ and of a magnitude of about 40 Mev for the s terms, while the depth of this potential hole should be of the order of several hundred Mev in order to produce a phase shift α_{33} of the observed magnitude. It is very questionable whether it is rewarding to adopt this potential model without a thorough study of its relativistic behavior.

5. From partial evidence on the scattering of pions by hydrogen previously reported,[8] a tentative conclusion had been reached that the states of isotopic spin $\frac{3}{2}$ are dominant. If this were exactly correct one would expect the cross sections for scattering of positive pions and for scattering of negative pions with and without charge exchange to be in the ratio 9:2:1 in all directions. That this is not so, is evident from a direct inspection of the cross sections which shows that the angular distribution for the scattering of positive pions and that of negative pions with charge exchange is mostly backward, whereas the elastic scattering of negative pions is mostly forward. Apparently this difference in angular distribution is due primarily to the phase shift α_1 of isotopic spin $\frac{1}{2}$ which is the largest phase shift with isotopic spin different from $\frac{3}{2}$.

On the assumption that the first solution is correct, the largest phase shift is α_{33} corresponding to a state for which the existence of a resonance has been suspected.[20] Our data do not extend far enough in energy to support the resonance hypothesis. If the hypothesis were correct, one would expect that at some higher energy the phase shift α_{33} should rise appreciably more rapidly than with the η^3 law and rather rapidly cross over from values less to values larger than 90°. It is possible, however, that α_{33} may go through a maximum and start decreasing before reaching 90°.

6. The present experimental data are utterly inadequate to allow any conclusions to be drawn about the d terms, which have been neglected in our analysis. If the interaction of the d levels were of the order of magnitude μc^2, the phase shifts would be a fraction of a degree. This makes our neglect of the d-terms justifiable but not necessarily correct.

This work could not have been carried out without the active cooperation and advice of Professor Earl A. Long. We thank him and Dr. Lothar Meyer for generous supplies of liquid hydrogen. Mr. Gaurang B. Yodh and Mr. Maurice Glicksman took an active part in the work of preparing the experimental equipment and carrying out the measurements; we are indebted to them for their time and skill. Mr. Leo Slattery contributed to the development of the electronic equipment. We are particularly grateful to Mr. Lester Kornblith for the efficient operation of the cyclotron.

[19] R. E. Marshak, Phys. Rev. **88**, 1208 (1952).

[20] K. A. Brueckner, Phys. Rev. **86**, 106 (1952).